The Penetration of Anticancer Drugs through Tumor Tissue as a Function of Cellular Adhesion and Packing Density of Tumor Cells

Rama Grantab, Shankar Sivananthan, and Ian F. Tannock

Division of Applied Molecular Oncology and Department of Medical Oncology and Hematology, Princess Margaret Hospital and University of Toronto, Toronto, Ontario, Canada

Abstract

To reach cancer cells in optimal quantities, therapeutic agents must be delivered to tumors through their imperfect blood vascular system, cross vessel walls into the interstitium, and penetrate multiple layers of tissue. Strategies to enhance drug penetration have potential to improve therapeutic outcome. The development of multicellular layers (MCLs), in which tumor cells are grown on a semipermeable Teflon support membrane, has facilitated quantification of drug penetration through solid tissue. The goals of the present study were to quantify the penetration of anticancer drugs as a function of cellular adhesion and packing density and to determine the effects of variable penetration on therapeutic efficacy in this model system. We compared the properties of MCLs grown from two epithelioid and round subclones of a colon carcinoma cell line. One pair of epithelioid and round sublines differed in expression of α-E-catenin, and both pairs generated MCLs with different packing density. The penetration of commonly used anticancer agents (paclitaxel, doxorubicin, methotrexate, and 5-fluorouracil) through MCLs derived from these cell lines was significantly greater through the round (loosely packed) than through the epithelioid (tightly packed) sublines. In MCLs treated with doxorubicin, we observed greater survival in the tightly packed cell lines than in the loosely packed cell lines. Impaired penetration of anticancer agents through MCLs derived from the tightly packed cell lines and relative resistance to killing of cells within them by doxorubicin treatment strengthen the role of tumor cell adhesion and packing density as contributing to drug resistance. (Cancer Res 2006; 66(2): 1033-9)

Introduction

The causes of drug resistance in solid tumors are multifactorial and most research has concentrated on genetic and cellular factors, which contribute to resistance of the individual cells. The proposed mechanisms of drug resistance in cancer are based largely on the study of drug-resistant variants isolated from tumor cells exposed to various classes of drugs in monolayer tissue culture. However, these methods of analysis tend to put little or no emphasis on physiologic mechanisms of drug resistance operative at the level of the whole tissue (1–4). To reach cancer cells in optimal quantities, a therapeutic agent must be delivered to a tumor through its imperfect blood vasculature, cross vessel walls into the interstitium, and penetrate multiple layers of solid tissue. This requirement may present a barrier to effective treatment and may be as important a cause of drug resistance as genetic and cellular factors (1–4).

Early studies of drug penetration through tissue employed multicellular spheroids, which provide a reasonable model for solid tumors with similarities of cellular environment including generation of an extracellular matrix and gradients of cell proliferation and nutrient concentration, gene expression, and biological behavior of cells (5–9). Studies using fluorescent or radiolabeled drugs have shown poor penetration of doxorubicin, vinblastine, paclitaxel, and methotrexate into the deeper layers of spheroids. Nevertheless, it is difficult to quantify drug penetration using the spheroid model.

An alternative model, the multicellular layer (MCL) model, developed by Wilson and his colleagues, provides a quantitative method that permits direct assessment of drug penetration through solid tissue (10, 11). Tumor cells are grown on collagen-coated microporous Teflon membranes. The resulting MCLs have a symmetrical, planar structure with tumorlike physiology. To examine penetration, a drug is added on one side of the MCL and its appearance on the other side of the MCL is measured as a function of time by appropriate analytic methods (Fig. 1). Like spheroids, MCLs share several properties with solid tumors derived from the same cell type, including a similar but not identical extracellular matrix and tight junctions between epithelial cells (12). Studies conducted in our laboratory and others have shown poor penetration of many commonly used anticancer drugs through MCLs generated from several human and murine cell lines (11–17). Drug penetration through MCLs was shown to be improved by agents that inhibit cellular uptake of anticancer drugs, suggesting that the penetration of chemotherapeutic agents is largely mediated by diffusion through the extracellular matrix (18, 19).

Previous studies using solid tumor histocultures and xenografts have shown poor drug penetration into solid tumors with high packing density (20), and drug penetration was shown to improve on administration of agents that induced apoptosis and reduction in cell density (20–22). The goals of the present study were to use the MCL model to quantify the penetration of anticancer drugs as a function of packing density of the cells and to determine the effect of drug penetration on therapeutic efficacy. We therefore compared the properties of MCLs grown from two different epithelioid clones of HCT-8 colon carcinoma cells and round subclones derived from each of them. The epithelioid and round sublines have different cell adhesion properties and generate MCLs with different packing density.

Requests for reprints: Ian F. Tannock, Department of Medical Oncology and Hematology, Princess Margaret Hospital, 610 University Avenue, Toronto, Ontario, Canada M5G 2M9. Phone: 416-946-2245; Fax: 416-946-2082; E-mail: ian.tannock@uhn.on.ca.

doi:10.1158/0008-5472.CAN-05-3077

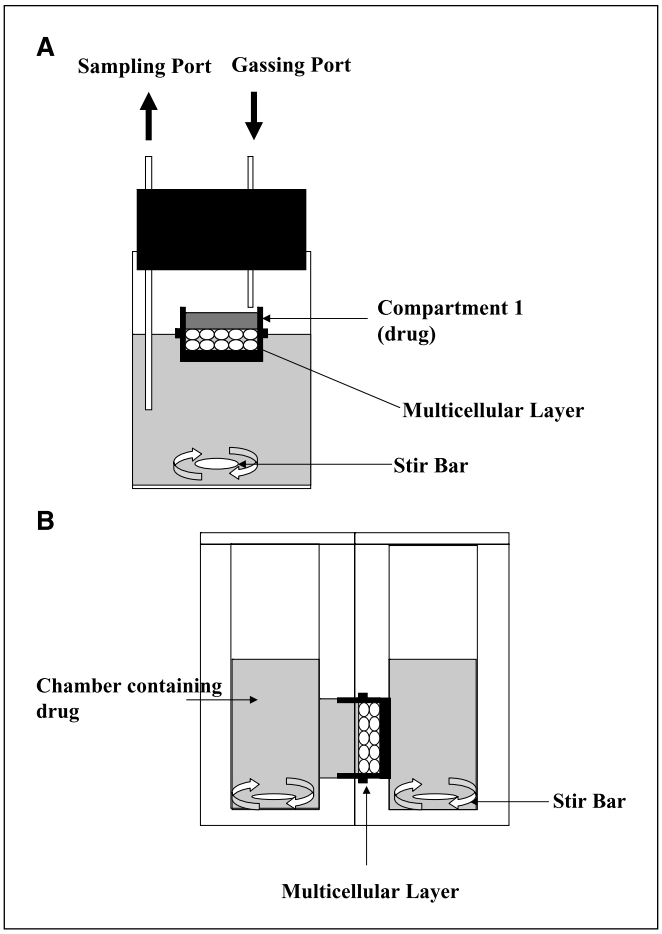

Figure 1. *A,* the experimental chamber used to assess drug penetration through a MCL. Anticancer agents dissolved in 1% agar (to prevent convection) are added to compartment 1 and the insert containing the drug and MCL is then floated in media. Samples are obtained from compartment 2 through the sampling port while the gas port delivers a mixture of 95% air and 5% CO_2. *B,* the dual chamber model avoids the use of agar and facilitates the disaggregation of cells in a MCL. In this system, drug at selected concentrations was dissolved in media in the chamber adjacent to the MCL.

'We have assessed the penetration of commonly used anticancer agents through MCLs derived from these cell lines and the ability of drugs to cause cellular toxicity within them. Our hypothesis is that penetration of drugs through tissue is inversely related to the packing density of cells and that impaired drug penetration will decrease drug toxicity for tumor cells within the tissue.

Materials and Methods

Cell lines. The HCT-8 cell lines consisted of epithelioid sublines and round variants that have been reported to possess a frame-shift mutation in the DNA repair gene *HMSH6* and heterozygosity for *CTNNA1* which codes for α-E-catenin (23). Due to this deficiency, round cells are unable to form adherens junctions and they generate MCLs with a large extracellular space whereas the parental epithelioid clones form tightly packed MCLs. The HCT-8 Ea and Ra sublines, referred to below as Ea and Ra sublines, were kindly provided by Dr. W.R. Wilson (Aukland Cancer Society Research Centre, University of Auckland, Auckland, New Zealand). These cells were grown as monolayers in α-MEM (Life Technologies, Inc., Burlington, ON, Canada) supplemented with 10% fetal bovine serum (FBS; Hyclone, Logan, UT) at 37° in a humidified atmosphere of 95% air plus 5% CO_2. The HCT-8/E11 and HCT-8/1R1 cell lines, referred to below as E11 and 1R1 sublines, were generously provided by Dr. M. Bracke (Ghent University Hospital, Gent, Belgium). These cells were grown as monolayers in RPMI medium (Life Technologies) containing 1 mmol/L pyruvate supplemented with 10% FBS. Cells were reestablished from frozen stock every 4 months and assessed periodically for the presence of *Mycoplasma*.

Growth and characterization of MCLs. Exponentially growing cells ($\sim 5 \times 10^5$) were seeded on collagen-coated, semiporous Teflon membrane culture inserts (Millipore, Bedford, MA). Briefly, 150 μL of collagen type III were dissolved in 0.01 mol/L HCl and diluted in a 1:4 ratio with 60% ethanol to a final concentration of 0.75 mmol/L; this was applied to the culture inserts and allowed to dry overnight. Cells were allowed to attach for 4 hours and the membranes were then submerged in a large volume of stirred α-MEM or RPMI medium containing 1 mmol/L pyruvate, supplemented with 10% FBS, and allowed to grow for 5 days. Uniformity of MCL growth was assessed using a light microscope; only MCLs with uniform growth across the membrane were used in experiments. To determine the number of cells in MCLs, one or more of them were selected at random, trypsinized, and the cells counted using a Coulter counter.

To characterize MCLs, they were fixed in 10% neutral buffered formalin for 24 hours and then processed through graded concentrations of ethanol (70%, 95%, and 100%). They were placed in xylene overnight and then embedded in paraffin and cut into 4-μm-thick sections. They were stained with H&E or Masson's trichrome to stain for extracellular matrix or with 4′,6-diamidino-2-phenylindole (DAPI) to quantify cellular packing density. DAPI-stained MCL sections were viewed with a Zeiss Axiovert 200M and packing density was quantified as the number of nuclei per unit surface area using Media Cybernetics Image Pro PLUS software.

Immunohistochemical staining for evaluation of matrix proteins was undertaken using a rabbit antilaminin polyclonal antibody (Sigma Chemical Co., St. Louis, MO) and human monoclonal antibodies against collagen type IV (DAKO Corp., Carpinteria, CA), fibronectin, E-cadherin, and β-catenin (all from BD Transduction Laboratories, Lexington, KY). Briefly, tissue sections were dewaxed in xylene and rehydrated through graded ethanol to water. Endogenous peroxidase activity was blocked with 3% aqueous hydrogen peroxide solution. Antigen retrieval was undertaken by pepsin digestion or heat retrieval. The slides were then incubated with the primary antibody for 1 hour at room temperature. Samples were washed in PBS and incubated for 30 minutes with either biotin antirabbit (Vector Laboratories, Burlingame, CA) or antimouse immunoglobulin G (IgG; Signet Pathology Systems, Inc., Dedham, MA) followed by 30-minute incubation with streptavidin-horseradish peroxidase complex (Signet Laboratories). Finally, the slides were counterstained lightly with Mayer's hematoxylin, dehydrated through alcohols, and mounted in Permount.

Western blotting for α-E-catenin. For Western blotting, MCLs were washed twice with ice-cold PBS and incubated with 500 μL of lysis buffer [50 mmol/L HEPES (pH 8.0), 10% glycerol, 1% Triton X-100, 150 mmol/L NaCl, 1 mmol/L EDTA, 1.5 mmol/L $MgCl_2$, 100 mmol/L NaF, 10 mmol NaP_2O_7, 1 mmol/L Na_3VO_4, and 1 tablet/7 mL protease inhibitor cocktail from Roche Diagnostics (Mannheim, Germany)] for 1 hour in 4°C. Lysates were cleared from the insoluble material and the resulting extracts were assayed for total protein content using a BCA Protein Assay Kit (Pierce, Rockford, IL). Equivalent quantities of protein were separated using 10% SDS-PAGE gels and subsequently transferred onto polyvinylidene difluoride membranes. Membrane blots were blocked overnight with TBS-Tween 20 containing 5% milk at 4°C. Membranes were probed at room temperature for 1 hour with rabbit polyclonal antibody against human α-E-catenin antibody (Sigma-Aldrich, St. Louis, MO). Blots were then incubated with horseradish peroxidase–linked antirabbit antibody (Amersham Biosciences, Baie d'Urfe, Quebec, Canada) for 1 hour at room temperature. Proteins were detected using enhanced chemiluminescence per instructions of the manufacturer (Amersham Biosciences). Blotting

Table 1. Characterization of MCLs derived from HCT-8 cell lines

	Doubling time of MCLs (h)	MCL thickness (layer with 3×10^6-5×10^6 cells), μm	Packing density (percentage of nuclear area ± SD)	Histologic morphology
HCT-8Ea	~42	~150	54.4 ± 4.6	Tightly packed; epithelioid morphology; fingerlike projections on MCL surface
HCT-8E11	~48	~200	50 ± 4.9	
HCT-8Ra	~28	~175	32.3 ± 3.8	Loosely packed; round morphology
HCT-81R1	~30	~230	39.3 ± 3.8	

with α-tubulin [monoclonal mouse IgG from Oncogene (San Diego, CA) and horseradish peroxidase–linked mouse IgG from Amersham Biosciences (Buckinghamshire, United Kingdom)] was used to control for protein loading. MCF-7 cells were used as a positive control.

Reverse transcription-PCR for α-E-catenin. Total RNA was extracted from MCF-7 cells (used as a control) and the HCT-8 Ea and Ra sublines using Qiagen RNeasy Mini Kit (Qiagen, Mississauga, Ontario, Canada) and subsequently treated with DNase (Ambion, Austin, TX) in accordance with the instructions of the manufacturer. Reverse transcription was conducted using DNase-treated total RNA mixed with anchored oligo-dT primer, 3′ RCPA (5′-AAGCAGTGGTATCAACCGCAGAGTAC-$(dT)_{26}$-3′), and deoxynucleotide triphosphates (dNTP; each of dATP, dCTP, dTTP, and dGTP at pH 7.0). The mixture was denatured at 65°C for 5 minutes and then immediately put on ice. Reverse transcription was done at 42°C for 2 hours in First-Strand Buffer [50 mmol/L Tris-HCl (pH 8.3) at room temperature, 75 mmol/L KCl, and 3 mmol/L $MgCl_2$] and dTT, in addition to 40 units of RNaseOUT and 250 units of SuperScript II RT (Invitrogen, Burlington, Ontario, Canada). PCR to detect α-catenin was conducted using the following primers as previously described by Oda et al. (24): primer S1, α-E-catenin-5′-CTTCGGGCCTCTGGAATTTA-3′ and primer A3, α-E-catenin-5′-CACCTGTTCCGCAATCTTCG-3′ (Invitrogen). The S1-A3 primer set was used for amplification of α-E-catenin cDNA between exons 1 and 13 as previously published by Oda et al. (24). PCR using S1 and A3 will produce a ~2,000-bp product. Glyceraldehyde-3-phosphate dehydrogenase (GAPDH) primers were used as controls for cDNA quality and RNA extracted from each cell line was used as a negative control. All PCR reactions were conducted using the following conditions: one cycle at 94°C for 3 minutes and 40 cycles at 94°C for 15 seconds, 53°C for 30 seconds, and 72°C for 30 seconds using a Platinum Taq Polymerase (Invitrogen) and a Platinum Taq DNA polymerase PCR buffer (Invitrogen) with 4 mmol/L Mg^{2+}, 400 nmol/L dNTPs, 400 nmol/L of primers, and 50 nmol/L probe in a total volume of 25 μL.

Anticancer drugs. [^{3}H]Paclitaxel (specific activity, 5 μCi/mmol/L) and [^{3}H]-5-fluorouracil (5-FU; specific activity, 10 μCi/mmol/L) were purchased from Maverik Biochemicals, Inc. (Brea, MA). [^{14}C]Doxorubicin (specific activity, 25 μCi/mmol/L) and [^{3}H]methotrexate (specific activity, 250 μCi/mmol/L) were purchased from Amersham Pharmacia Biotech (Amersham, United Kingdom) and [^{14}C]sucrose (specific activity, 50 μCi/mmol/L) was obtained from Perkin-Elmer Life Sciences, Inc. (Boston, MA). Unlabeled doxorubicin (Pharmacia, Mississauga, Ontario, Canada), paclitaxel (Bristol-Myers Squibb, Montreal, Quebec, Canada), 5-FU, and methotrexate (both from Mayne Pharma, Montreal, Quebec, Canada) were obtained in their clinical formulations.

Penetration of anticancer drugs. Solutions containing radiolabeled anticancer drugs were prepared in 2× α-MEM (without FBS) and mixed in a 1:1 ratio with 1% agar solution. A volume of 0.5 mL of this mixture was added to one side of the MCL (compartment 1, Fig. 1*A*); the 1% agar solution was included to prevent convection. MCLs were then floated on 18 mL of stirred culture media (compartment 2, Fig. 1*A*). A cell-free tissue culture insert was included in all experiments as a control. Experiments were conducted at 37°C in glass vials exposed to 95% air/5% CO_2. The appearance of drugs in compartment 2 as a function of time was assessed by liquid scintillation counting of 150 μL samples withdrawn from compartment 2. Drug penetration through MCLs is presented as a ratio of C/C_∞, where C is the measured drug concentration and C_∞ represents the calculated concentration of the drug when it has equilibrated between the two compartments. [^{14}C]Sucrose was included as an internal standard at a concentration of 3 μmol/L in all experiments, except those conducted with [^{14}C]doxorubicin; only MCLs with a maximum variation of ±20% in sucrose penetration were used for analysis. To minimize statistical variation, experiments conducted with [^{14}C]doxorubicin were repeated four times and only MCLs with total cell numbers ranging from 3×10^6 to 4.5×10^6 were used to assess doxorubicin penetration.

The initial concentration of drugs in compartment 1 was as follows: 25 μmol/L paclitaxel, 5 μmol/L doxorubicin, 10 μmol/L methotrexate, and 77 μmol/L 5-FU. These concentrations approximate those that can be achieved in serum after *in vivo* administration and permit sensitive detection of the drug in compartment 2; they were achieved using a mixture of radiolabeled and unlabeled drugs.

Fluorescent micrographs of drug penetration were obtained by treating MCLs derived from each subline with 10 μmol/L using a dual chamber reservoir apparatus (Fig. 1*B*). MCLs were then fixed in 10% neutral buffered formalin and processed as previously described under low light conditions. Images were obtained using Zeiss Axiovert 200M with Roper Scientific Coolsnap HQ.

Clonogenic assays. The sensitivity of each cell line to methotrexate, doxorubicin, 5-FU, and paclitaxel was assessed in a clonogenic assay. Exponentially growing cells were exposed for 24 hours to various doses of chemotherapeutic agents in monolayer. Cells were then trypsinized, washed twice, and serial dilutions were plated in six-well plates with each well containing 5 mL of media. The sublines showed sensitivity only to doxorubicin and this drug was selected for further experiments.

MCLs containing 3×10^6 to 5×10^6 cells were exposed at 37°C to varying concentrations of doxorubicin for 24 hours in a dual reservoir apparatus in which drugs were added to stirred media on one side of the MCL (Fig. 1*B*). The dual chamber apparatus was used instead of the vertical chamber to avoid the use of agar and thereby to facilitate disaggregation and subsequent plating of cells. After treatment, MCLs were disaggregated by pipetting, trypsinized, and washed twice. Serial dilutions were plated as described above. Plates were incubated for 10 days (Ra and 1R1 cells) or 14 days (Ea and E11 cells) at 37°C in 95% air/5% CO_2 and 90% humidity. Cells were then stained with methylene blue and colonies containing >50 cells were counted.

Cell cycle distribution. MCLs were disaggregated by pipetting, trypsinized, washed twice, and resuspended in PBS at 1×10^6 cells/mL. Cells from MCLs and single-cell suspensions were incubated with 1 μmol/L propidium iodide containing 0.1% Triton X-100 (Pierce) and 50 mg/mL RNase (Qiagen, Inc., Mississauga, Ontario, Canada) for 30 minutes. Multicycle AV software version 2.5 (Phoenix Flow Systems, San Diego, CA) was used for cell cycle analysis.

Statistical analysis. Data for drug penetration and for cell survival are presented as mean ± SE for at least three replicate experiments.

Comparisons between data for HCT-8/R and HCT-8/E cell lines were analyzed using SigmaPlot software. Statistical significance was based on two-sided t tests with $P_s < 0.05$.

Results

Characterization of cell lines and MCLs. Properties of the cell lines are summarized in Table 1. Cells within MCLs derived from the Ea and E11 cells displayed epithelial morphology with close contact between cells and the formation of fingerlike projections on the surface of the MCLs (Fig. 2*A* and *C*). In contrast, Ra and 1R1 cells formed loosely packed MCLs with significantly lower cell concentration than those derived from the corresponding Ea and E11 cells (Fig. 2*B* and *D*).

Immunohistochemical assessment of the extracellular matrix of MCLs derived from the sublines indicated the presence of laminin in all cell lines but no staining for collagen IV or fibronectin. Although laminin distribution was observed throughout the MCLs, its deposition was particularly evident on the MCL surface and especially along the fingerlike projections of the MCLs formed from the E11 and Ea sublines.

Western blot analysis showed no α-E-catenin expression in the 1R1 subline, but surprisingly, expression was similar in both Ea and Ra sublines (Fig. 3*A*). Using reverse transcription-PCR (RT-PCR) analysis with the S1 and A3 primer set, *α-E-catenin* mRNA splicing in the Ra subline between exons 1 to 13 was similar to that in the Ea subline (Fig. 3*B*). Immunohistochemical analysis showed expression of E-cadherin and β-catenin in all sublines (data not shown).

Drug penetration through MCLs. The penetration of all anticancer drugs tested was slower through the MCLs than through the cell-free Teflon membrane (Fig. 4; Table 2); their penetration was also greater through MCLs derived from the loosely packed Ra and 1R1 sublines than through MCLs derived from the corresponding tightly packed Ea or E11 sublines.

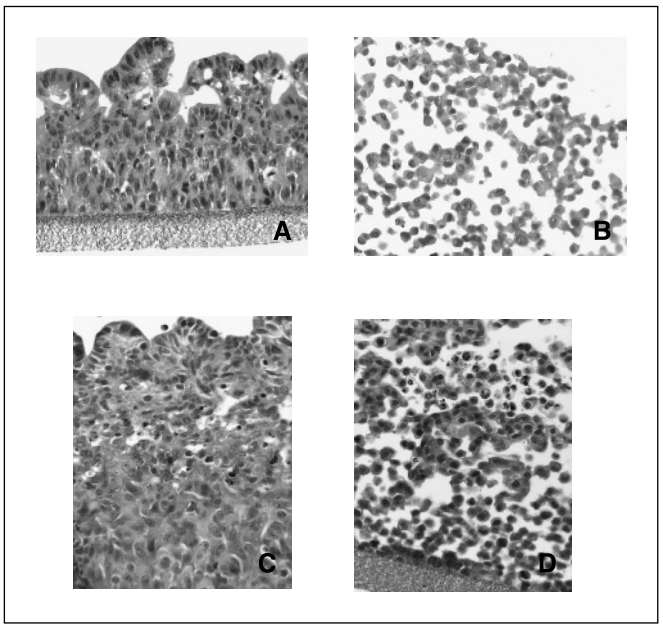

Figure 2. H&E-stained sections of MCLs derived from the HCT-8 sublines: Ea (*A*), Ra (*B*), E11 (*C*), and 1R1 (*D*).

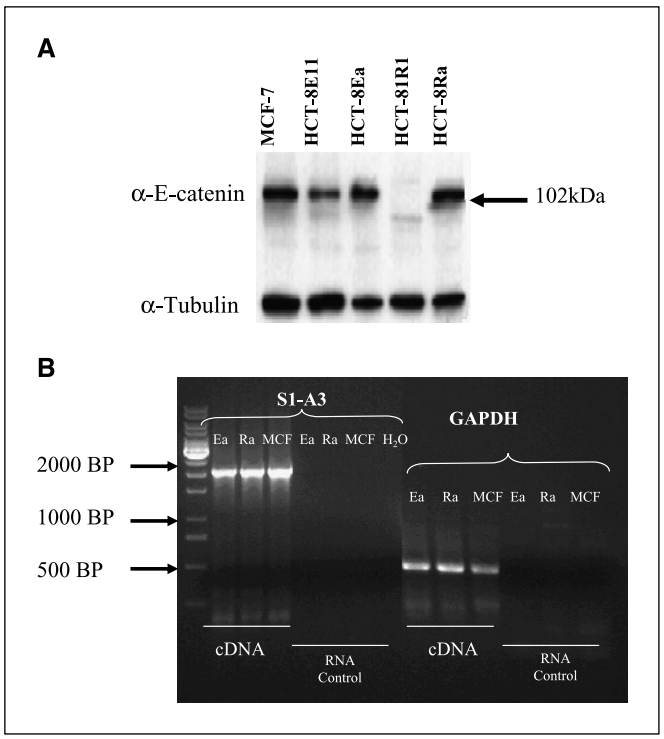

Figure 3. Analysis of α-E-catenin expression in HCT-8 sublines. MCF-7 cells served as a positive control in Western blot and RT-PCR experiments. *A,* expression of α-E-catenin (102 kDa) as assessed by Western blotting. *B,* further assessment of α-E-catenin using RT-PCR. RT-PCR was conducted using primers S1-A3 (27). The S1-A3 primer set produces a product of 2,109 bp (which spans exons 1-13). The presence of a band at 2,109 bp suggests no aberrant splicing of *α-E-catenin* mRNA in the Ea and Ra sublines. RT-PCR products for GAPDH were produced using primers specific for GAPDH and were included as a control.

Fluorescent micrographs of doxorubicin penetration through MCLs derived from Ea and E11 sublines show that, at 15 minutes, penetration is limited to the peripheral cell layers whereas, at 6 hours, doxorubicin penetration involves ~1/3 of the MCL (Fig. 5). In MCLs derived from the Ra and R1 sublines, drug penetration is initially restricted to the outer cell layers (those adjacent to the drug containing chamber) whereas, at 6 hours posttreatment, doxorubicin fluorescence is prominent in all cell layers and the outer cell layers have begun to dissociate from the MCL. At 24 hours posttreatment, the outer cell layers dissociate from the MCL; this disaggregation was especially prominent in the MCLs derived from the R1 subline (Fig. 5).

Sensitivity to doxorubicin. Survival curves for cells in monolayer and for cells in the corresponding MCLs treated with doxorubicin for E11 and 1R1 sublines are shown in Fig. 6. Cells in monolayer are more sensitive than cells in MCLs with no significant difference in sensitivity between the sublines in monolayer. Cells in the more loosely packed MCLs derived from the Ra and 1R1 cell lines were considerably more sensitive than those in MCLs derived from the corresponding tightly packed Ea and E11 cell lines (P = 0.014 for Ea and Ra and P = 0.048 for E11 and 1R1).

Flow cytometric DNA analysis showed that ~14.2 ± 1.2% and 16.9 ± 2.9% of MCLs derived from E11 and 1R1 cells, respectively, were in the S phase. Hence, variations in cytotoxicity between the two cell lines were not likely to be due to differences in the percentage of S-phase cells between MCLs derived from these cells.

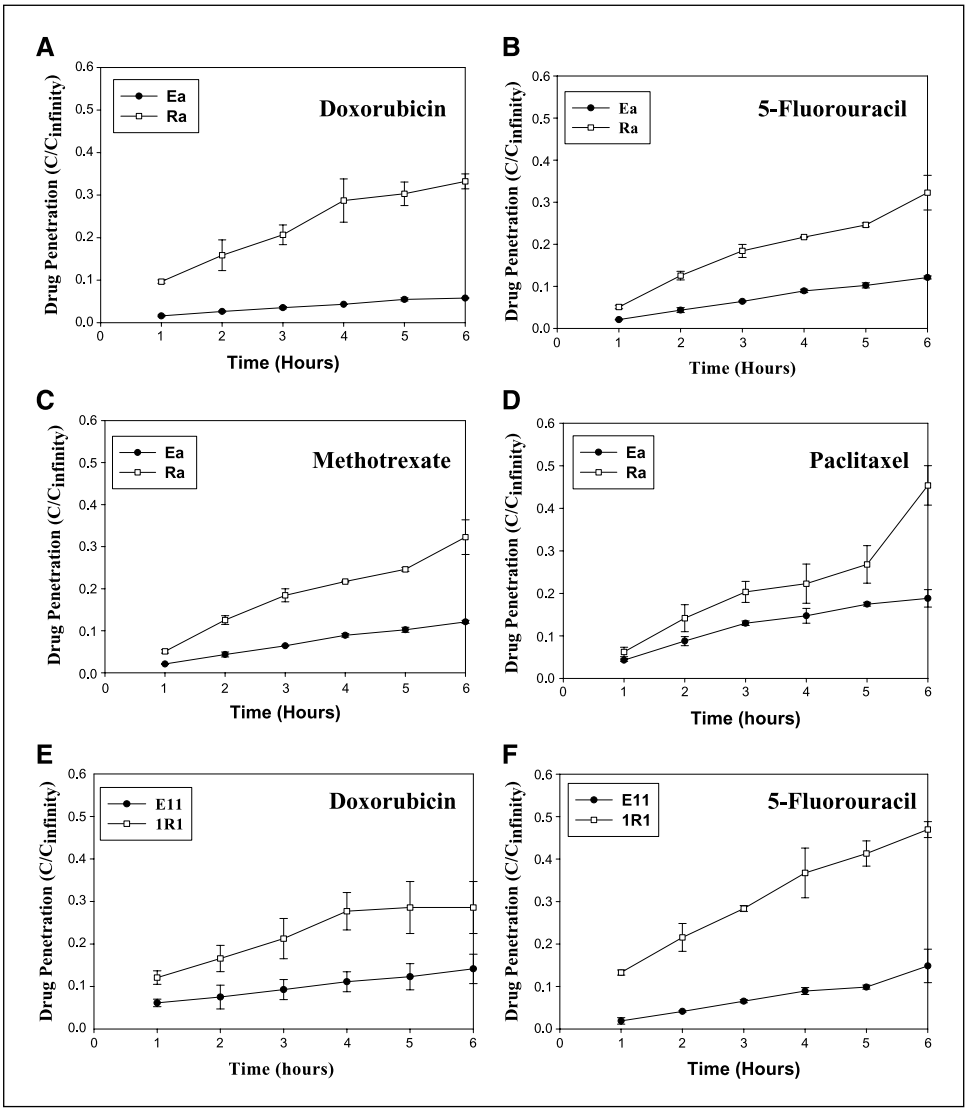

Figure 4. Penetration of anticancer drugs as a function of time through MCLs derived from human colon carcinoma cell lines. *Symbols,* ratio of radiolabeled drug concentration in compartment 2 (*C*) to the concentration of drug at equilibrium ($C_{infinity}$). *A* to *D,* drug penetration through Ea and Ra sublines. The penetration of doxorubicin (*A*), 5-FU (*B*), methotrexate (*C*), and paclitaxel (*D*) was assessed in MCLs containing 3.5×10^6 to 5×10^6 cells. *E* and *F,* doxorubicin and 5-FU penetration through E11 and 1R1 sublines, respectively. [^{14}C]Sucrose was used as an internal control in experiments, except those conducted with doxorubicin. *Points,* mean of three or more experiments; *bars,* SD. Where the error bars are not readily evident, the SD was lower than the width of the symbols.

Discussion

The present study illustrates that the packing density and adhesive properties of cells may influence drug penetration and toxicity in solid tumors. Using two sets of colon carcinoma cell lines and commonly used antineoplastic agents, we have shown an inverse correlation between tumor packing density and drug penetration. Penetration of radiolabeled drugs across the MCLs was assessed by quantifying the concentration of radiolabel in the receiving compartment; we recognize that radiolabel might be associated with a metabolite; thus, this provides an upper limit for the rate of penetration of the parent compound through the MCLs.

Visualization of doxorubicin penetration through MCLs established from E11 and R1 sublines shows that, initially, drug penetration is limited to the periphery of the MCLs (adjacent to the drug-containing chamber). Although the penetration of doxorubicin increases over the course of 24 hours, the level of drug penetration is greater through the loosely packed than through the tightly packed MCLs. These observations are further supported by the differences in cytotoxicity that were observed after 24 hours of treatment with doxorubicin: higher levels of survival in the tightly packed MCLs derived from Ea colon cancer and HCT-8E11 cells. The disaggregation of proximal layers of MCLs derived from 1R1 and Ra sublines (Fig. 5, *bottom right*) after treatment with doxorubicin might facilitate further penetration of the drug into the deeper layers of the MCLs. Our data support the role of tumor microenvironment in limiting drug penetration and thereby in causing effective drug resistance.

The cell lines used in this study consisted of two tightly packed and two loosely packed cell lines. Quantification of packing density and characterization of the tightly and loosely packed sublines did not reveal morphologic differences between Ea and E11 and between Ra and 1R1 sublines. Because Ea and Ra sublines were obtained as HCT-8 sublines and previous studies have shown that the transition from the epithelioid to the round morphotype is due to a mutation in the second allele of *α-E-catenin,* the expression of α-E-catenin in the Ra subline was unexpected (23, 25). Our experiments to characterize the adhesion defect in the Ra subline did not reveal differences in the expression of E-cadherin or other extracellular matrix

Table 2. Penetration of anticancer drugs through MCLs derived from each cell line and through the coated Teflon membrane alone at 6 hours

Cell line	Doxorubicin	5-Fluorouracil	Paclitaxel	Methotrexate
Ea	12.3 ± 1.0	12.1 ± 0.6	18.8 ± 2.1	5.78 ± 0.02
E11	14.1 ± 3.5	14.8 ± 3.9		
Ra	55.1 ± 3.2	32.3 ± 7.1	45.4 ± 4.6	33.2 ± 3.0
1R1	35.8 ± 4.5	46.9 ± 1.9		
Cell-free	84.1 ± 5.4	80.3 ± 8.5	58.4 ± 1.6	45.1 ± 8.0

NOTE: Percent drug penetration is obtained from the ratio of the drug concentration in compartment 2 (at 6 hours) to drug concentration at equilibrium ± SD. Data represent results from three to five experiments. Penetration of paclitaxel and methotrexate was not studied in MCLs derived from E11 and 1R1 cell lines.

components. Although the nature of the molecular mechanisms leading to the transition from Ea to Ra has not been elucidated, the morphologic differences (including packing density and response to chemotherapeutic agents) observed between the Ea and Ra sublines were similar to those found in the E11 and 1R1 sublines.

The majority of *in vitro* studies of drug resistance focus on mechanisms that operate at the level of the single cell. Assessment of cellular behavior in monolayer cultures *in vitro* has contributed to the understanding of the role of DNA repair/apoptotic pathways, drug target alterations, and multidrug resistance mediated by drug efflux pumps in drug resistance (4, 26, 27). However, monolayer systems disregard the contribution of tumor physiology, particularly cell-cell interactions, the extracellular matrix, and tumor microenvironment, to chemotherapeutic resistance. Both Ea and E11 sublines show slightly greater sensitivity to doxorubicin than Ra and 1R1 sublines when treated in monolayer. Our data also show greater cell killing in monolayer than in multilayers for all concentrations tested and, in contrast to monolayers, better cell killing in the loosely packed MCLs derived from Ra and 1R1 cells than the corresponding tightly packed MCLs. Whereas drug consumption in the MCLs might have some effect on their effective drug exposure as a function of time, this is likely to be small, and will apply to MCLs derived from each of the sublines. Our findings are in agreement with other studies that have shown that some types of drug resistance are expressed only in three-dimensional tissue; they provide evidence for the role of tumor architecture, particularly packing density, in drug resistance of solid tumors.

Strategies that modify or alter solid tumor physiology have been shown to improve the cytotoxicity of several antineoplastic agents. Studies conducted by St. Croix et al. (28) have shown that treatment with hyaluronidase increases the susceptibility of spheroids derived from EMT-6 mammary carcinoma cells to treatment with 4-hydroxycyclophosphamide as compared with untreated spheroids. The authors conclude that hyaluronidase acts as an antiadhesive agent that leads to spheroid disaggregation and increased chemosensitivity. These experiments suggest that specific interactions between cancer cells and their environment (cell-cell as well as cell-matrix adhesion) ultimately contribute to the outcome of chemotherapy. Sherman-Baust et al. (29) have shown up-regulation of collagen VI in cisplatin-resistant ovarian cancer spheroids whereas studies by Netti et al. (30) have shown that tumors with a well-defined collagen network are more resistant to penetration of macromolecules (such as IgG) compared with tumors that exhibit a loose collagen network. Collagenase treatment of the tumors, leading to the degradation of collagen, was shown to enhance the diffusion coefficient of index molecules through these tumors, providing further evidence for the role of tumor microenvironment as a barrier to drug penetration. In addition, modification

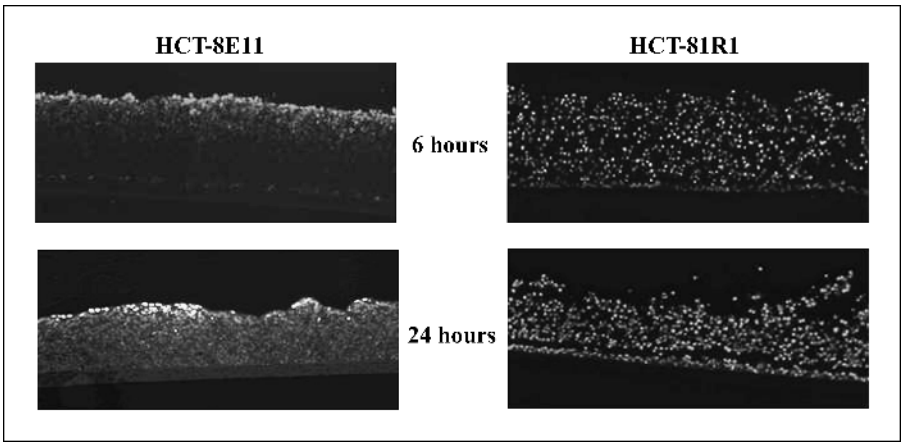

Figure 5. Penetration of doxorubicin through MCLs derived from E11 and 1R1 sublines after 6 and 24 hours. Doxorubicin penetration is slower through MCLs derived from the tightly packed E11 cell line with distribution of the drug largely in the proximal layers. Similar patterns were observed using Ea and Ra sublines although, at 24 hours posttreatment, less MCL disaggregation was observed for these cell lines than for the E11 and 1R1 subtypes.

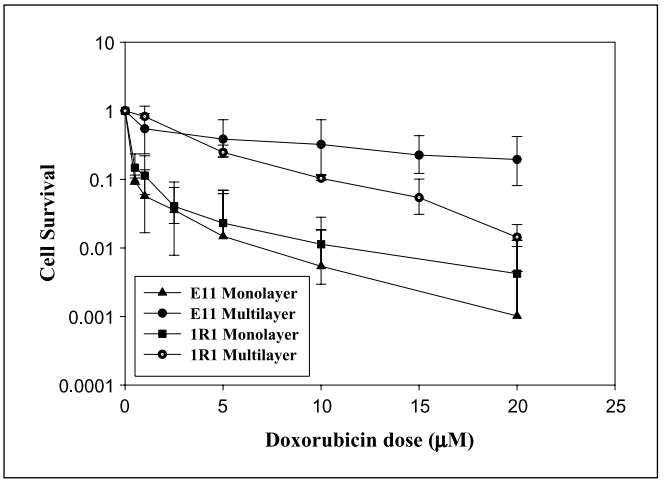

Figure 6. Clonogenic assays conducted using HCT-8E11 and HCT-81R1 cells exposed to varying concentrations of doxorubicin in monolayers or MCLs for 24 hours. Cell survival is presented as the ratio of colonies at a particular drug concentration to colonies in the untreated condition. *Points,* mean from three experiments; *bars,* SD. Similar results were obtained using Ea and Ra sublines (data not shown).

of tumor packing density using pretreatment schedules with doxorubicin or paclitaxel for 24 hours reduced cell density and improved the distribution of highly protein-bound drugs in solid tumors (21, 22).

In conclusion, our findings support the role of the tumor microenvironment in drug resistance in solid tumors. We have shown that tumor packing density poses a barrier to effective drug penetration, which will in turn decrease chemotherapeutic cytotoxicity. Future studies will focus on modifying cell packing density to improve the penetration of index drugs and hence drug activity

Acknowledgments

Received 8/29/2005; revised 11/4/2005; accepted 11/9/2005.

The costs of publication of this article were defrayed in part by the payment of page charges. This article must therefore be hereby marked *advertisement* in accordance with 18 U.S.C. Section 1734 solely to indicate this fact.

We thank the staff of the Advanced Optical Microscopy Facility, University health network for allowing us use of their computerized image analysis equipment; the staff at the Pathology Research Program at Toronto General Hospital and James Ho for assistance with immunohistochemistry; Baiwei Gong and Francis Tong for their technical assistance; and Drs. W.R. Wilson and M. Bracke for kindly providing us with the HCT-8 sublines.

References

1. Jain RK. Vascular and interstitial barriers to delivery of therapeutic agents in tumors. Cancer Metastasis Rev 1990;9:253–66.
2. Jain RK. Transport of molecules, particles, and cells in solid tumors. Annu Rev Biomed Eng 1999;1:241–63.
3. Tannock IF. Tumor physiology and drug resistance. Cancer Metastasis Rev 2001;20:123–32.
4. Cole SPC, Tannock IF. The Basic Science of Oncology. 4th ed. New York (NY): McGraw-Hill Companies, Inc.; 2005. p. 376–99.
5. Sutherland RM, Eddy HA, Bareham B, Reich K, Vanantwerp D. Resistance to Adriamycin in multicellular spheroids. Int J Radiat Oncol Biol Phys 1979;5:1225–30.
6. West GW, Weichselbaum R, Little JB. Limited penetration of methotrexate into human osteosarcoma spheroids as a proposed model for solid tumor resistance to adjuvant chemotherapy. Cancer Res 1980; 40:3665–8.
7. Nederman T, Carlsson J. Penetration and binding of vinblastine and 5-fluorouracil in cellular spheroids. Cancer Chemother Pharmacol 1984;13:131–5.
8. Sutherland RM. Cell and environment interactions in tumor microregions: the multicell spheroid model. Science 1988;240:177–84.
9. Durand RE. Distribution and activity of antineoplastic drugs in a tumor model. J Natl Cancer Inst 1989;81: 1623–52.
10. Hicks KO, Ohms SJ, van Zijl PL, Denny WA, Hunter PJ, Wilson WR. An experimental and mathematical model for the extravascular transport of a DNA intercalator in tumours. Br J Cancer 1997;76:894–903.
11. Wilson WR, Hicks KO. Measurement of extravascular drug diffusion in multicellular layers. Br J Cancer 1999; 79:1623–6.
12. Tannock IF, Lee CM, Tunggal JK, Cowan DS, Egorin MJ. Limited penetration of anticancer drugs through tumor tissue: a potential cause of resistance of solid tumors to chemotherapy. Clin Cancer Res 2002;8:878–84.
13. Hicks KO, Fleming Y, Siim BG, Koch CJ, Wilson WR. Extravascular diffusion of tirapazamine: effect of metabolic consumption assessed using the multicellular layer model. Int J Radiat Oncol Biol Phys 1998;42:641–9.
14. Phillips RM, Loadman PM, Cronin BP. Evaluation of a novel *in vitro* assay for assessing drug penetration into avascular regions of tumours. Br J Cancer 1998;77:2112–9.
15. Tunggal JK, Cowan DS, Shaikh H, Tannock IF. Penetration of anticancer drugs through solid tissue: a factor that limits the effectiveness of chemotherapy for solid tumors. Clin Cancer Res 1999;5:1583–6.
16. Kyle AH, Minchinton AI. Measurement of delivery and metabolism of tirapazamine to tumour tissue using the multilayered cell culture model. Cancer Chemother Pharmacol 1999;43:213–20.
17. Kyle AH, Huxham LA, Chiam AS, Sim DH, Minchinton AI. Direct assessment of drug penetration into tissue using a novel application of three-dimensional cell culture. Cancer Res 2004;64:6304–9.
18. Tunggal JK, Melo T, Ballinger JR, Tannock IF. The influence of expression of P-glycoprotein on the penetration of anticancer drugs through multicellular layers. Int J Cancer 2000;86:101–7.
19. Cowan DS, Tannock IF. Factors that influence the penetration of methotrexate through solid tissue. Int J Cancer 2001;91:120–5.
20. Au JL, Jang SH, Wientjes MG. Clinical aspects of drug delivery to tumors. J Control Release 2002;78:81–95.
21. Kuh HJ, Jang SH, Wientjes MG, Weaver JR, Au JL. Determinants of paclitaxel penetration and accumulation in human solid tumor. J Pharmacol Exp Ther 1999; 290:871–80.
22. Jang SH, Wientjes MG, Au JL. Enhancement of paclitaxel delivery to solid tumors by apoptosis-inducing pretreatment: effect of treatment schedule. J Pharmacol Exp Ther 2001;296:1035–42.
23. Vermeulen SJ, Nollet F, Teugels E, et al. The αE-catenin gene (CTNNA1) acts as an invasion-suppressor gene in human colon cancer cells. Oncogene 1999;18: 905–15.
24. Oda T, Kanai Y, Shimoyama Y, Nagafuchi A, Tsukita S, Hirohashi S. Cloning of the human α-catenin cDNA and its aberrant mRNA in a human cancer cell line. Biochem Biophys Res Commun 1993;193:897–904.
25. Vanpoucke G, Nollet F, Tejpar S, Cassiman JJ, van Roy F. The human αE-catenin gene CTNNA1: mutational analysis and rare occurrence of a truncated splice variant. Biochim Biophys Acta 2002;1574:262–8.
26. Gottesman MM. Mechanisms of cancer drug resistance. Annu Rev Med 2002;53:615–27.
27. Longley DB, Johnston PG. Molecular mechanisms of drug resistance. J Pathol 2005;205:275–92.
28. St. Croix B, Rak JW, Kapitain S, Sheehan C, Graham CH, Kerbel RS. Reversal by hyalurodinase of adhesion dependent multicellular drug resistance in mammary carcinoma cells. J Natl Cancer Inst 1996; 88:1285–96.
29. Sherman-Baust CA, Weeraratna AT, Rangel LB, et al. Remodeling of the extracellular matrix through overexpression of collagen VI contributes to cisplatin resistance in ovarian cancer cells. Cancer Cell 2003;3: 377–86.
30. Netti PA, Berk DA, Swartz MA, Grodzinsky AJ, Jain RK. Role of extracellular matrix assembly in interstitial transport in solid tumors. Cancer Res 2000;60: 2497–503.

The Penetration of Anticancer Drugs through Tumor Tissue as a Function of Cellular Adhesion and Packing Density of Tumor Cells

Rama Grantab, Shankar Sivananthan and Ian F. Tannock

Cancer Res 2006;66:1033-1039.